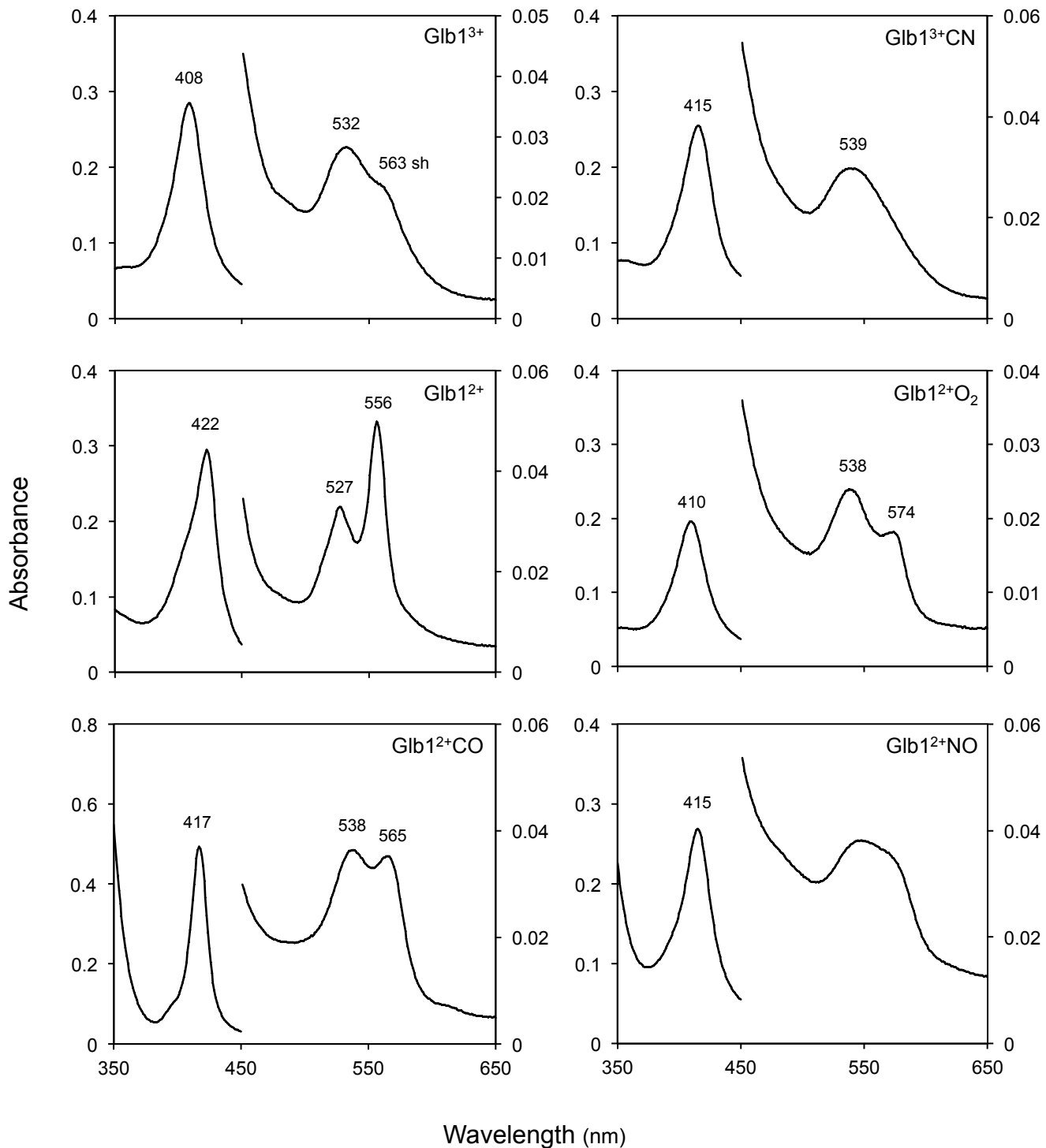


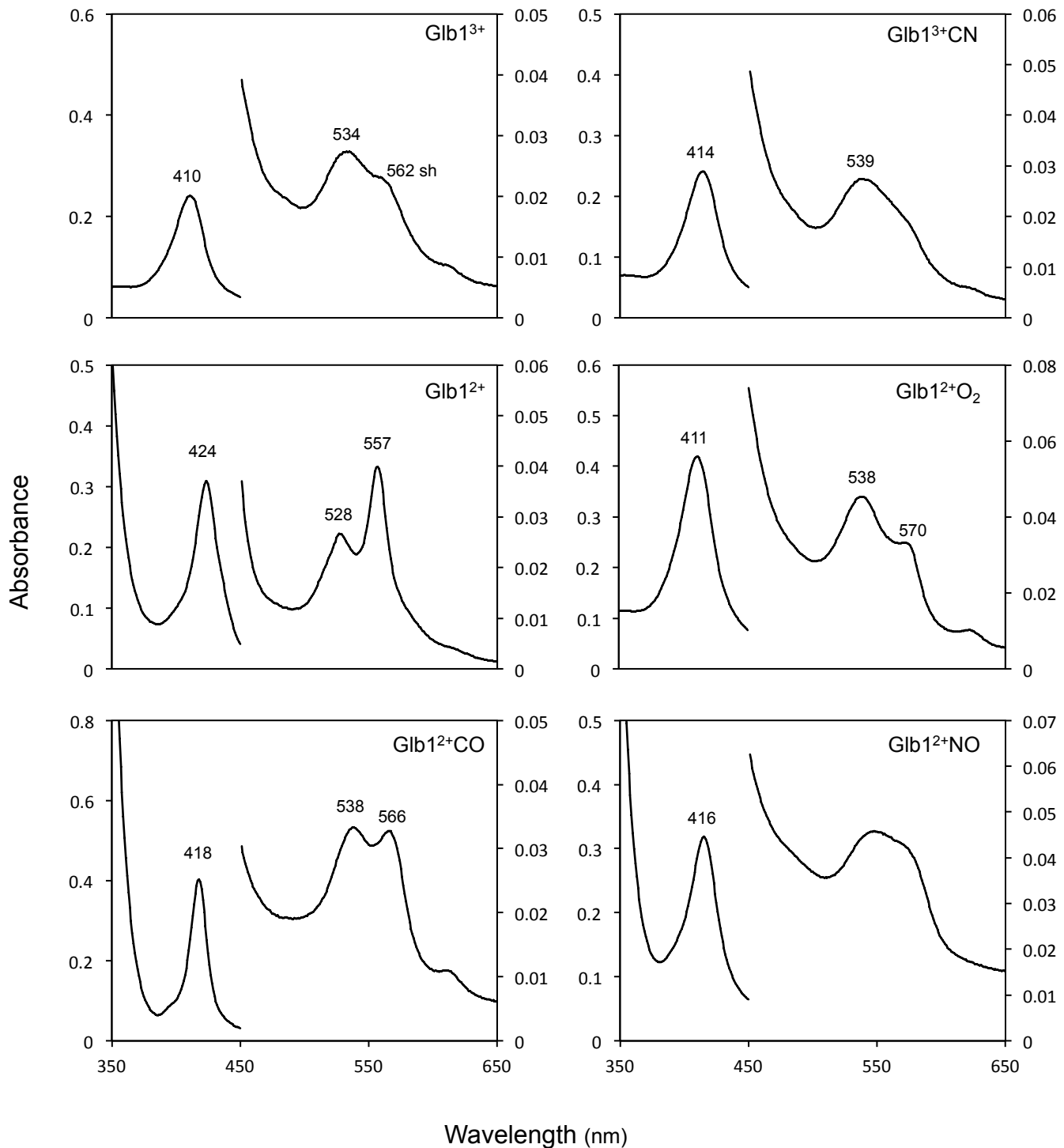
FIGURE S1 | Alignment of the four proteins encoded by the *MtGlb1-2* gene with typical class 1 Glbs of *Arabidopsis thaliana* and legumes. Highlighted in blue are the distal His residues. Alignment was performed with Clustal Omega from EMBL-EBI (<https://www.ebi.ac.uk/Tools/msa/clustalo/>). Abbreviations and accession numbers: Atha, *Arabidopsis thaliana* (At2g16060); Ljap, *Lotus japonicus* (Lj3g3v3338170); Mtru, *Medicago truncatula* (Medtr4g068860); Tpra, *Trifolium pratense* (PNX93138); Cari, *Cicer arietinum* (Ca_13651); Lang, *Lupinus angustifolius* (OIV99463); Gmax, *Glycine max* (Glyma.11G121800); Pvul, *Phaseolus vulgaris* (Phvul.011G048700); Vung, *Vigna unguiculata* (XP_027910775).

FIGURE S2 | UV-Visible spectra of MtGlb1-2.1 and MtGlb1-2.4 proteins with HT. (A) WT1, (B) 74, (C) 238, (D) 74/238, (E) WT4 and (F) 109. For each Glb, the figure shows the spectra of the ferric form (3+), the deoxyferrous form (2+), the complex of ferric globin with cyanide (3+CN), and the complexes of ferrous globin with O₂ (2+O₂), CO (2+CO) and NO (2+NO). The spectra of WT1 and WT4 were obtained with *c.* 18 μM protein in 50 mM potassium buffer (pH 7.0). The spectra of the mutants were obtained with *c.* 18 μM protein in the same buffer supplemented with 150 mM NaCl. *sh*, shoulder.

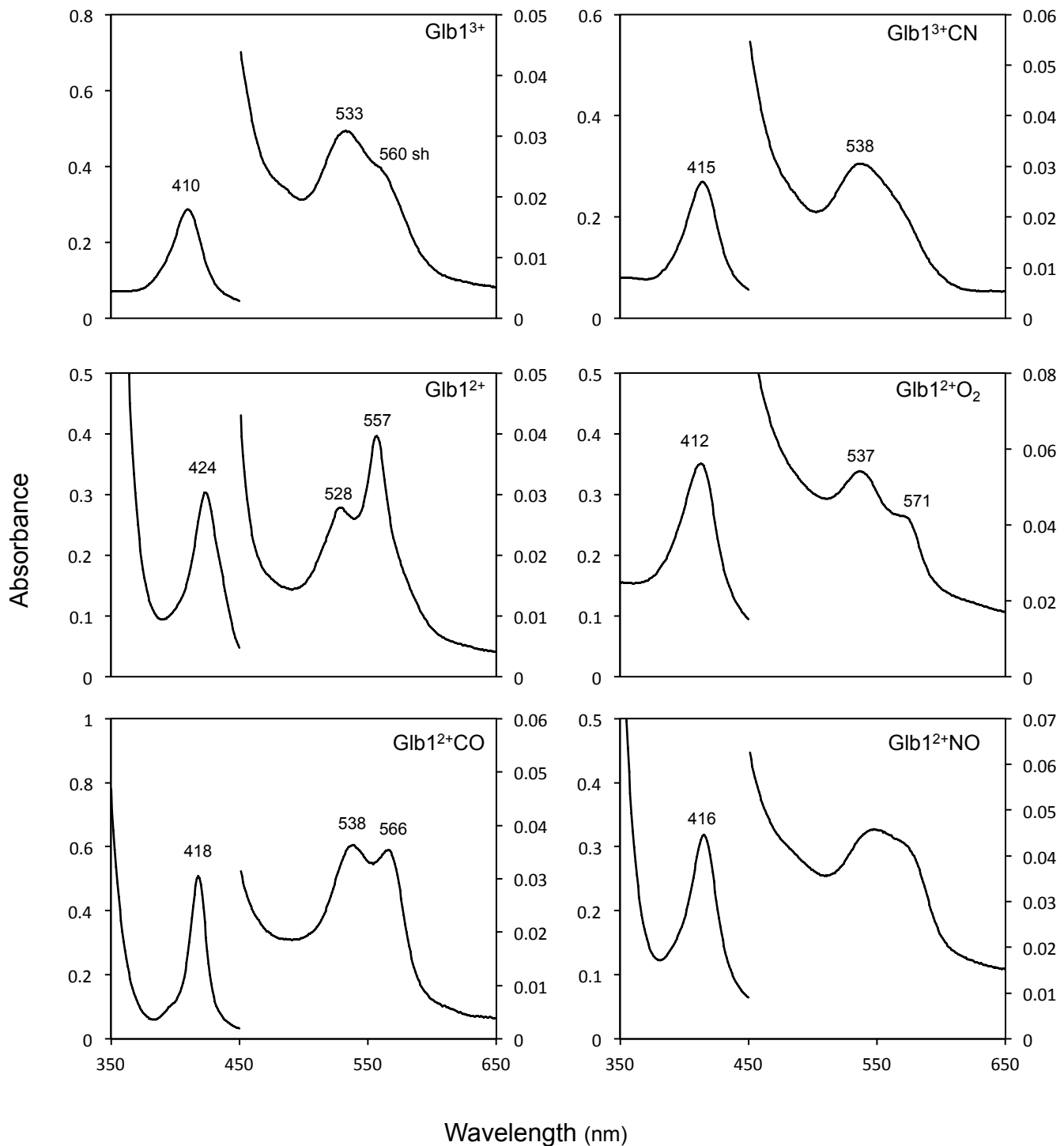
A MtGlb1-2.1 WT1 (HT)



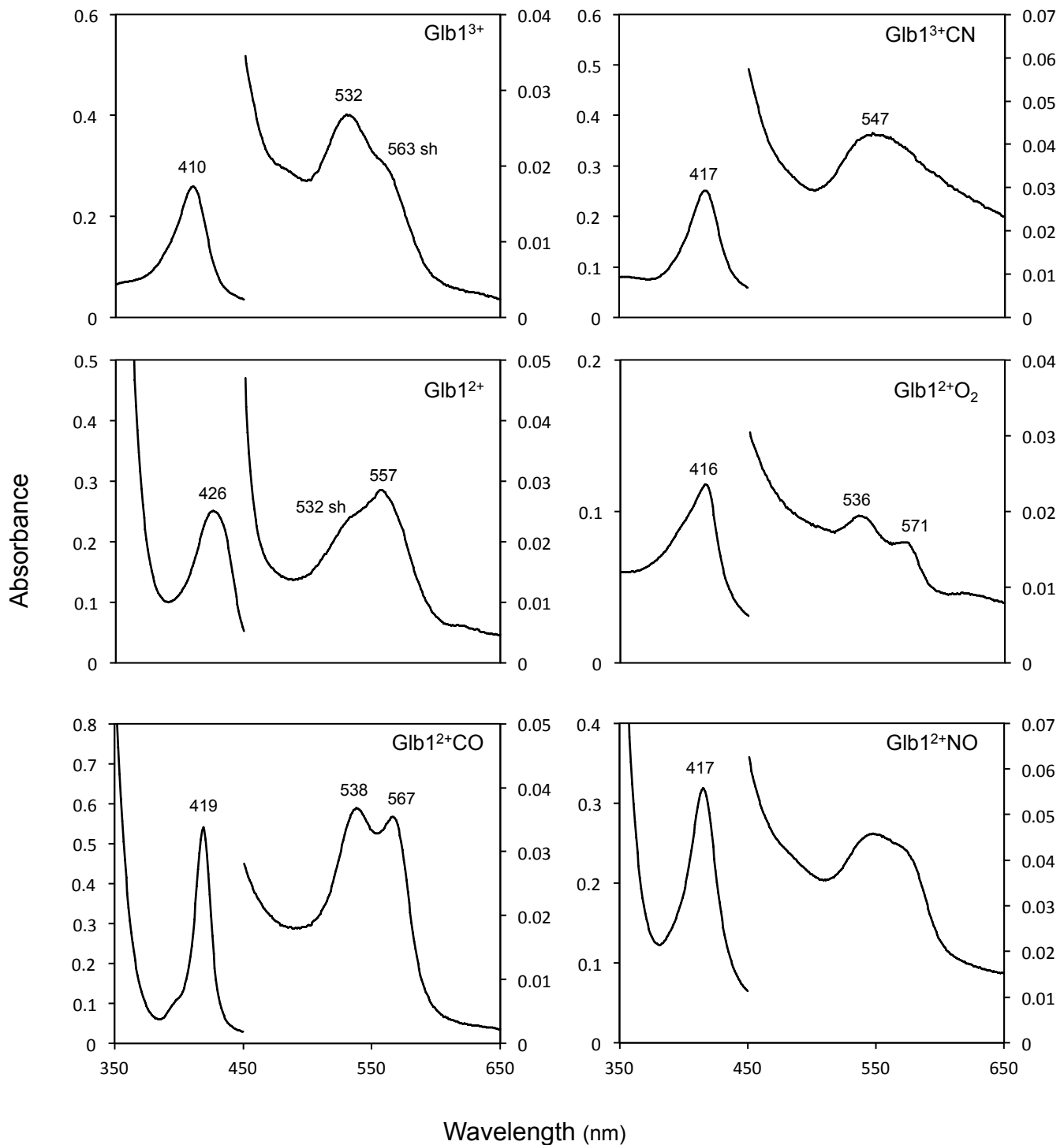
B MtGlb1-2.1 H74L (HT)



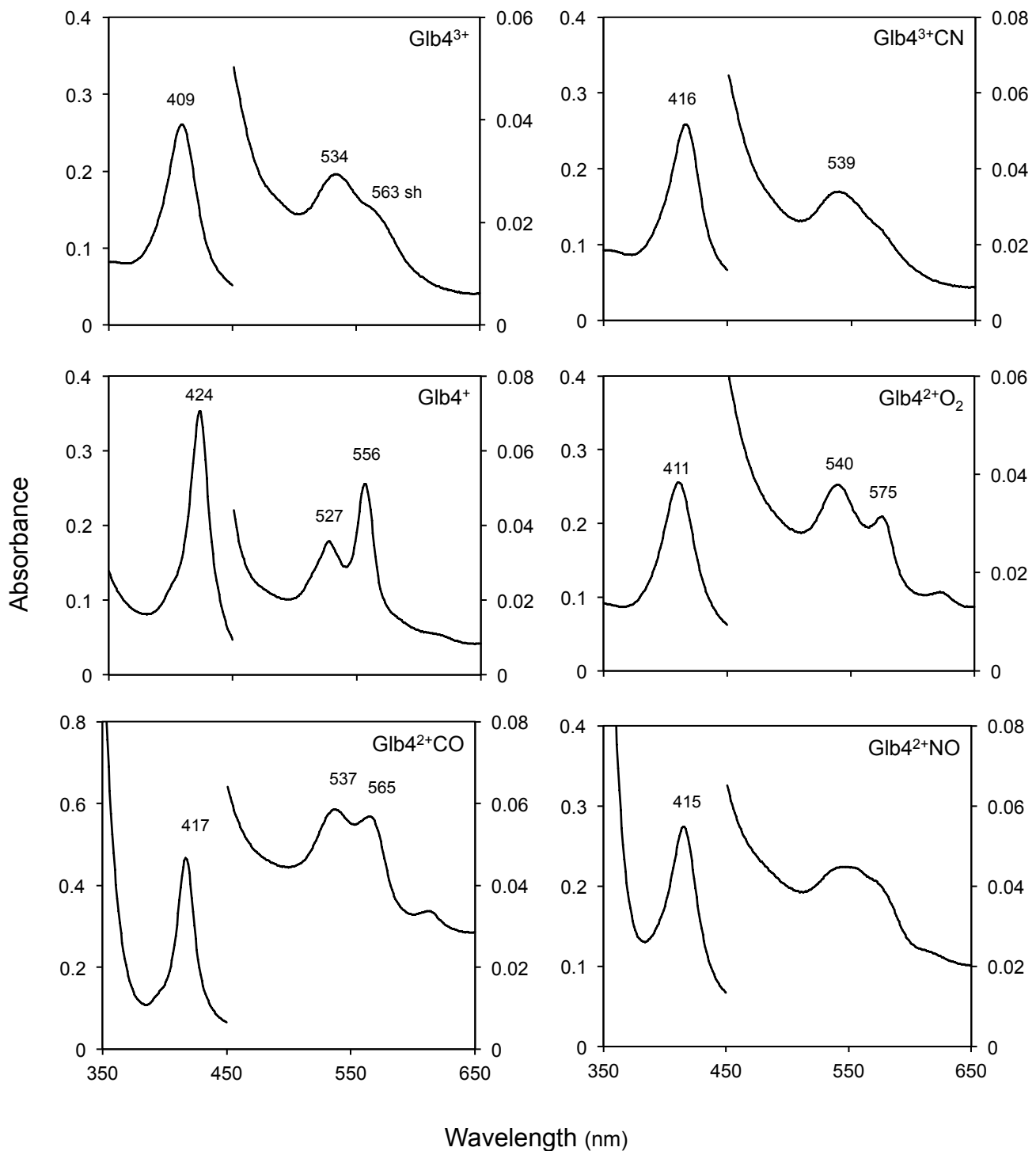
C MtGlb1-2.1 H238L (HT)



D MtGlb1-2.1 H74L / H238L (HT)



E MtGlb1-2.4 WT4 (HT)



F MtGlb1-2.4 H109L (HT)

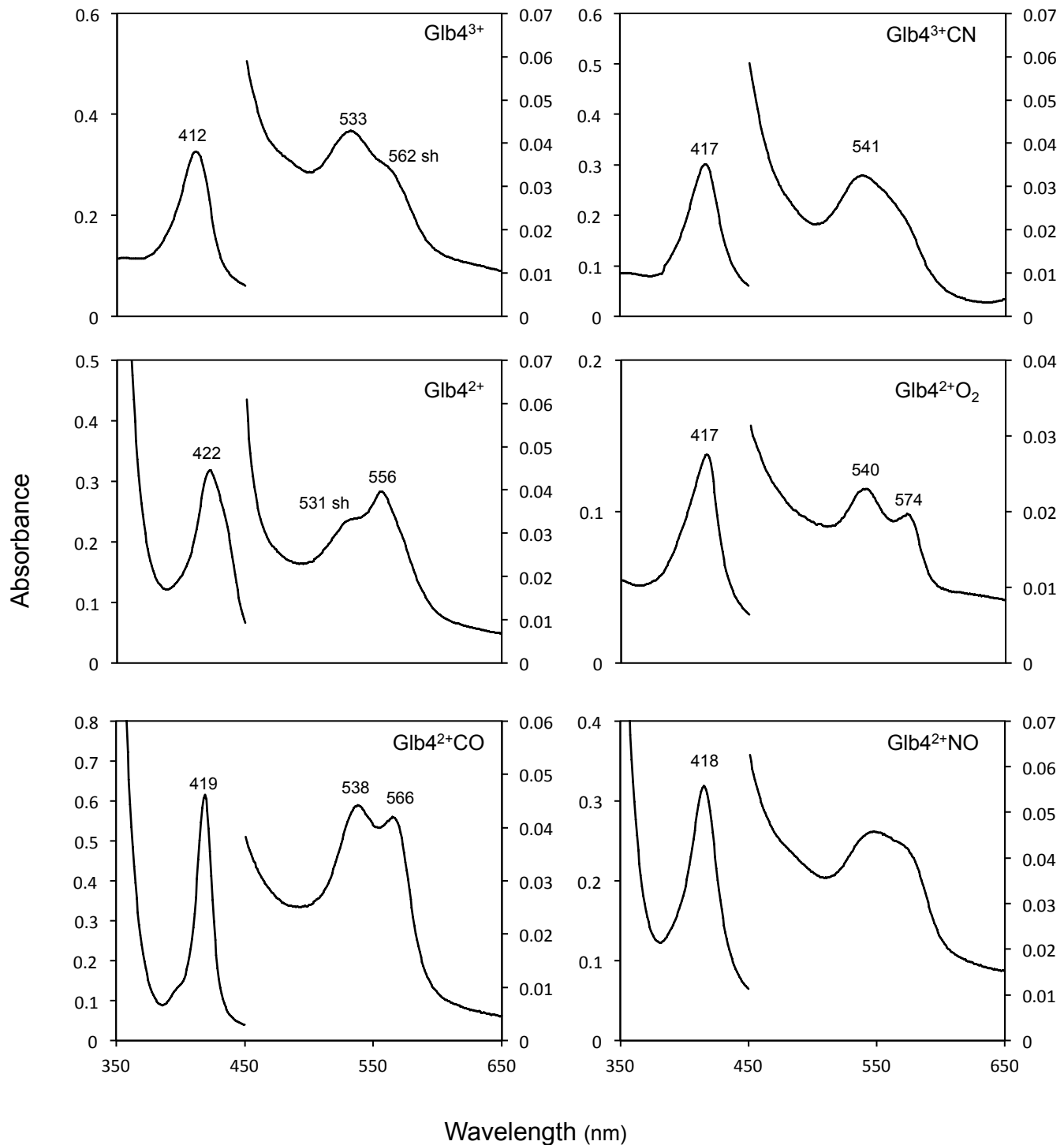
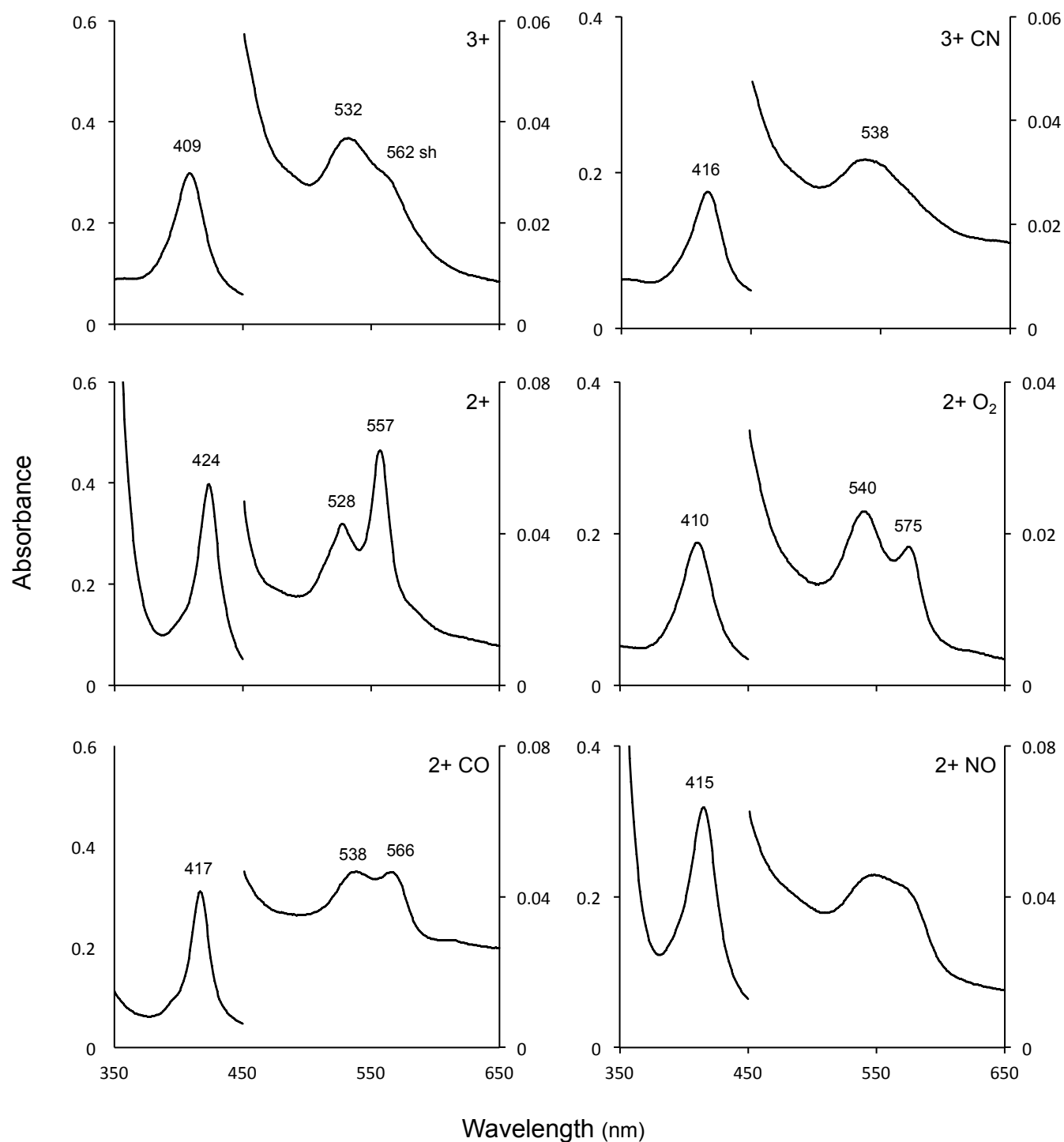
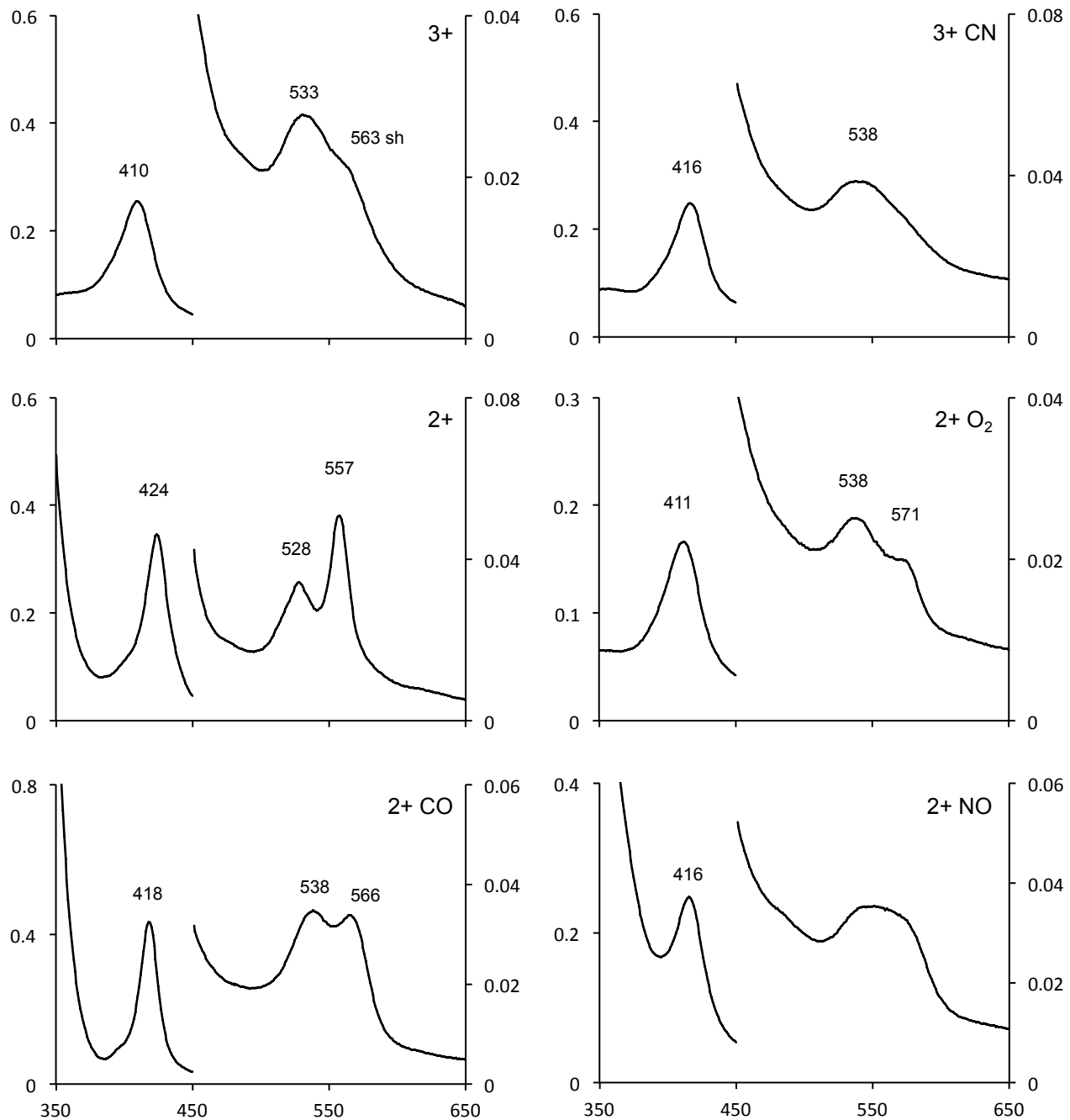


FIGURE S3 | UV-Visible spectra of MtGlb1-2.1 with Strep-tag (ST). (A) WT1, (B) 74, (C) 238 and (D) 74/238. For each globin, the figure shows the spectra of the ferric form (3+), the deoxyferrous form (2+), the complex of Glb³⁺ with cyanide (3+CN), and the complexes of Glb²⁺ with O₂ (2+O₂), CO (2+CO) and NO (2+NO). The spectra of WT1 were obtained with *c.* 20 μM globin in 50 mM potassium buffer (pH 7.0). The spectra of the mutants were obtained with *c.* 20 μM globin in the same buffer supplemented with 150 mM NaCl. *sh*, shoulder.

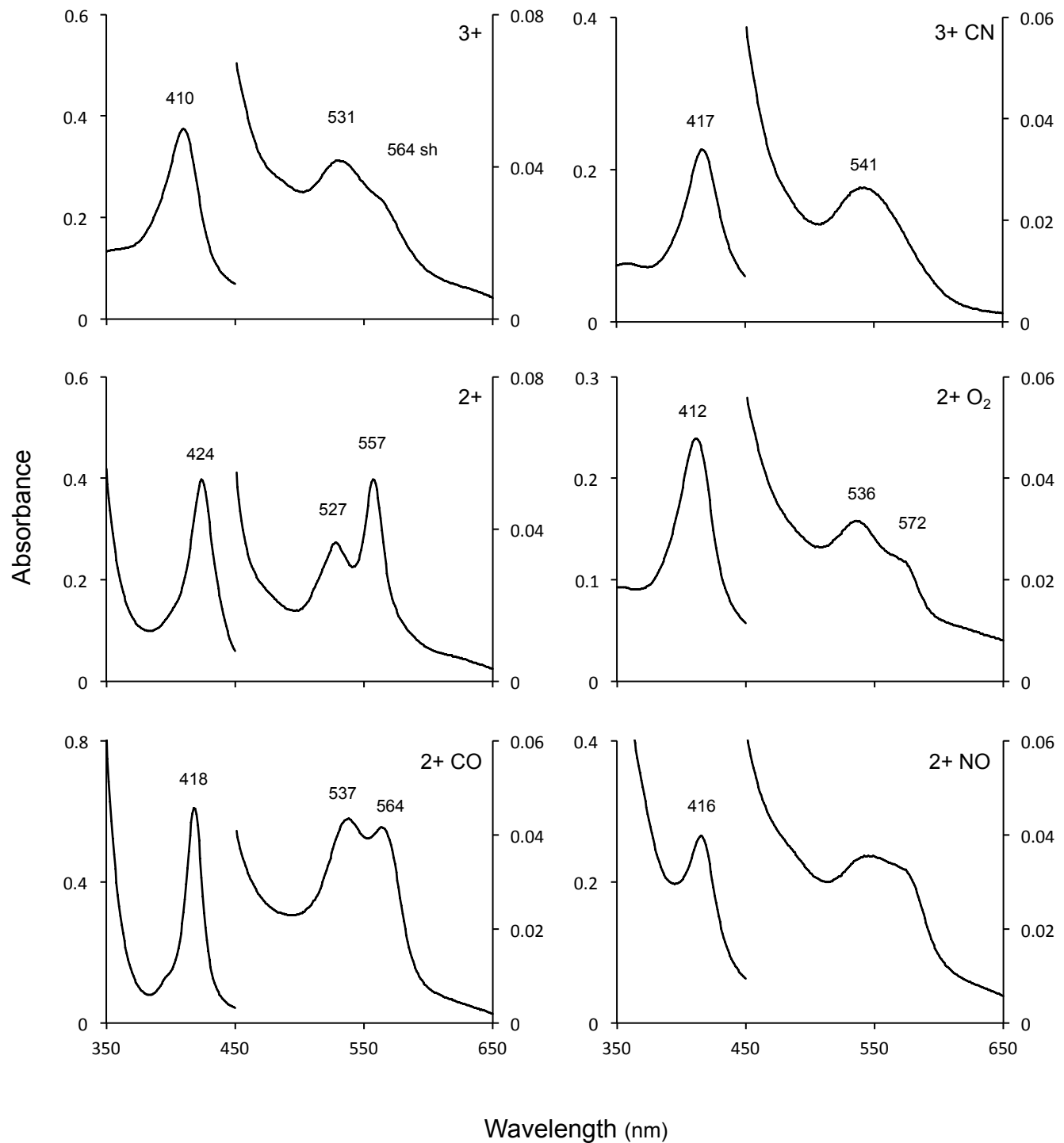
A MtGlb1-2.1 WT1 (ST)



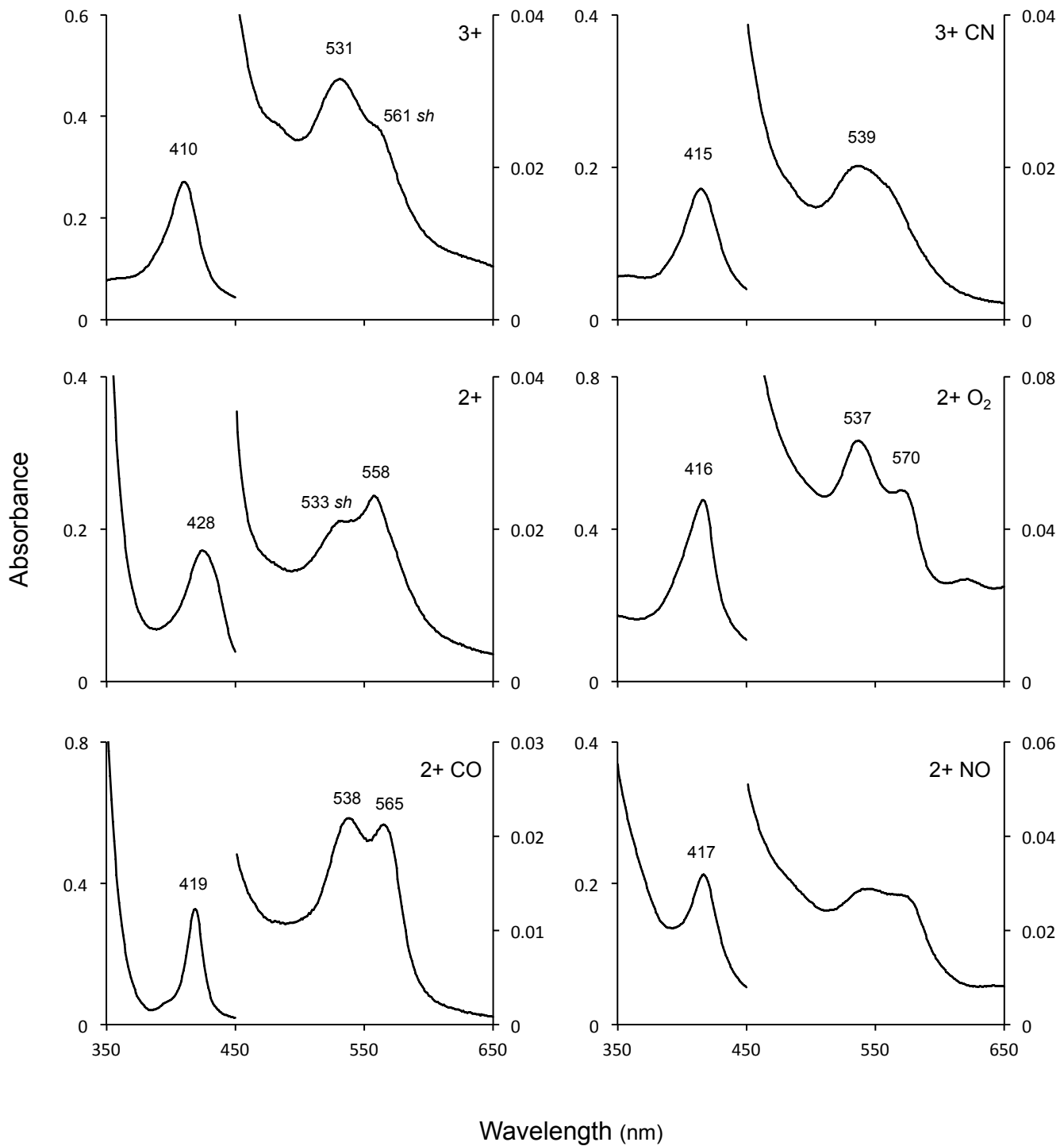
B MtGlb1-2.1 74 (ST)



C MtGlb1-2.1 238 (ST)



D MtGlb1-2.1 74/238 (ST)



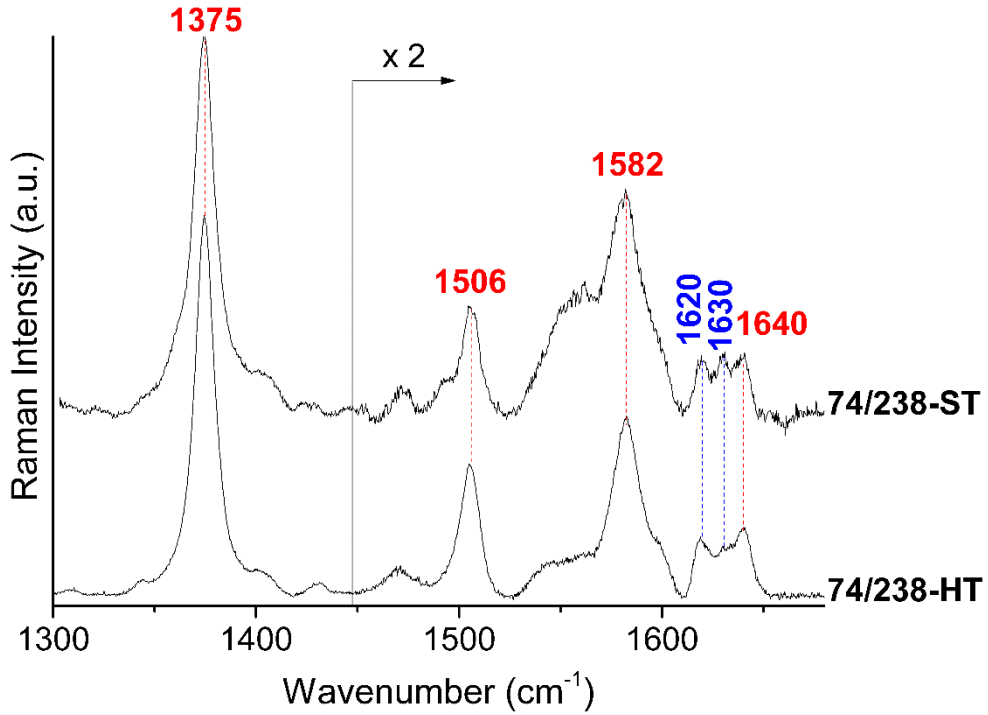


FIGURE S4 | High-frequency region RR spectra of the ferric 74/238 mutant purified with His-tag (HT) and Strep-tag (ST). The spectra have been shifted along the y -axis and the $1450\text{--}1700\text{ cm}^{-1}$ region has been expanded two-fold for better visualization. Experimental conditions: excitation at 406.7 nm , laser power at the sample 5 mW , average of four spectra with 40 min integration time (74/238 HT) or average of six spectra with 30 min integration time (74/238 ST).

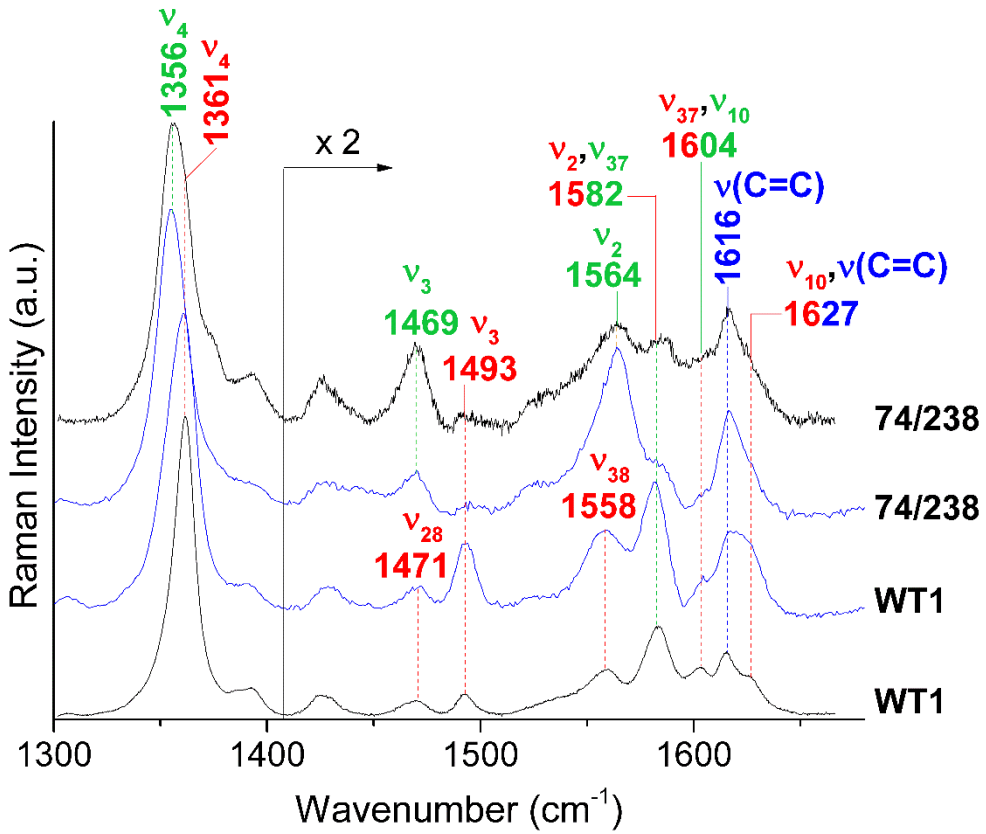


FIGURE S5 | High-frequency region RR spectra of deoxyferrous WT1 and 74/238. The spectra were obtained with excitation at 413.1 nm (black traces), in resonance with the 6cLS species, and excitation at 441.6 nm (blue traces), in resonance with the 5cHS species. The wavenumbers of the core size marker bands of the 6cLS and 5cHS species and the vinyl $\nu(\text{C}=\text{C})$ stretching modes are reported in red, green, and blue, respectively. The spectra have been shifted along the y-axis and the 1430–1700 cm^{-1} region has been expanded two-fold for better visualization. Experimental conditions at 413.1 nm: laser power at the sample 5 mW, average of three spectra with 30 min integration time (all proteins). Experimental conditions at 441.6 nm: laser power at the sample 10 mW, average of four spectra with 12 min integration time (WT1), average of four spectra with 10 min integration time (74/238).

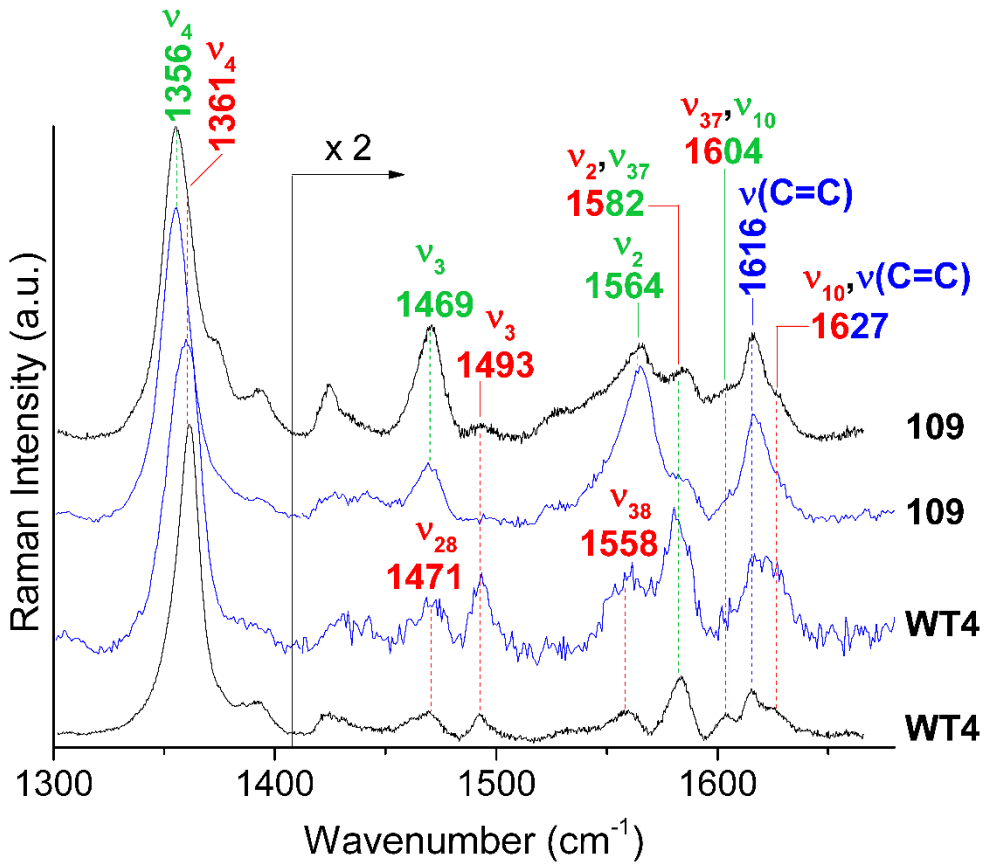


FIGURE S6 | High-frequency region RR spectra of deoxyferrous WT4 and 109. The spectra were obtained with excitation at 413.1 nm (black traces), in resonance with the 6cLS species, and excitation at 441.6 nm (blue traces), in resonance with the 5cHS species. The wavenumbers of the core size marker bands of the 6cLS and 5cHS species and the vinyl $\nu(\text{C}=\text{C})$ stretching modes are reported in red, green, and blue, respectively. The spectra have been shifted along the y-axis and the $1430\text{--}1700\text{ cm}^{-1}$ region has been expanded two-fold for better visualization. Experimental conditions at 413.1 nm: laser power at the sample 5 mW, average of three spectra with 30 min integration time (all proteins). Experimental conditions at 441.6 nm: laser power at the sample 10 mW, average of three spectra with 9 min integration time (WT4), average of six spectra with 18 min integration time (109).

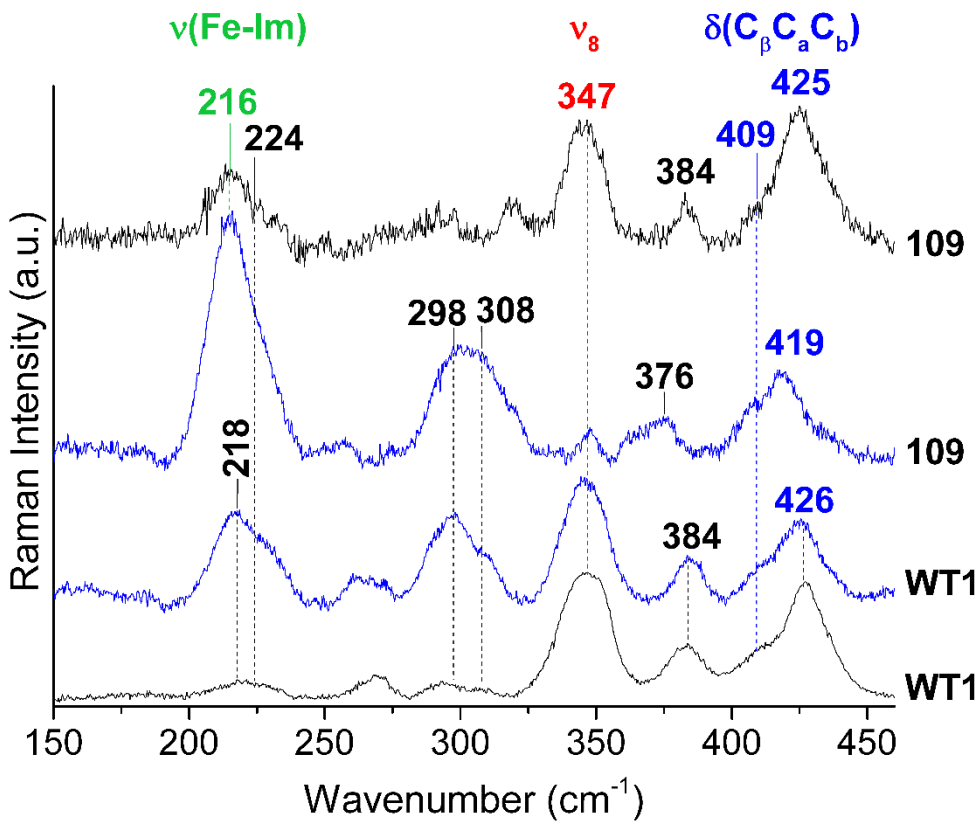


FIGURE S7 | Low-frequency region RR spectra of deoxyferrous WT1 and 109. The spectra were obtained with excitation at 413.1 nm (black traces), in resonance with the 6cLS species, and excitation at 441.6 nm (blue traces), in resonance with the 5cHS species. The wavenumbers of the marker bands of the 6cLS and 5cHS species and the vinyl $\delta(C_b C_a C_b)$ bending modes are reported in red, green and blue, respectively. The spectra have been shifted along the y -axis for better visualization. Experimental conditions with excitation at 413.1 nm: laser power at the sample 5 mW, average of four spectra with 40 min integration time (WT1), average of three spectra with 30 min integration time (109). Experimental conditions with excitation at 441.6 nm: laser power at the sample 10 mW, average of six spectra with 60 min integration time (WT1) and average of three spectra with 30 min integration time (109).

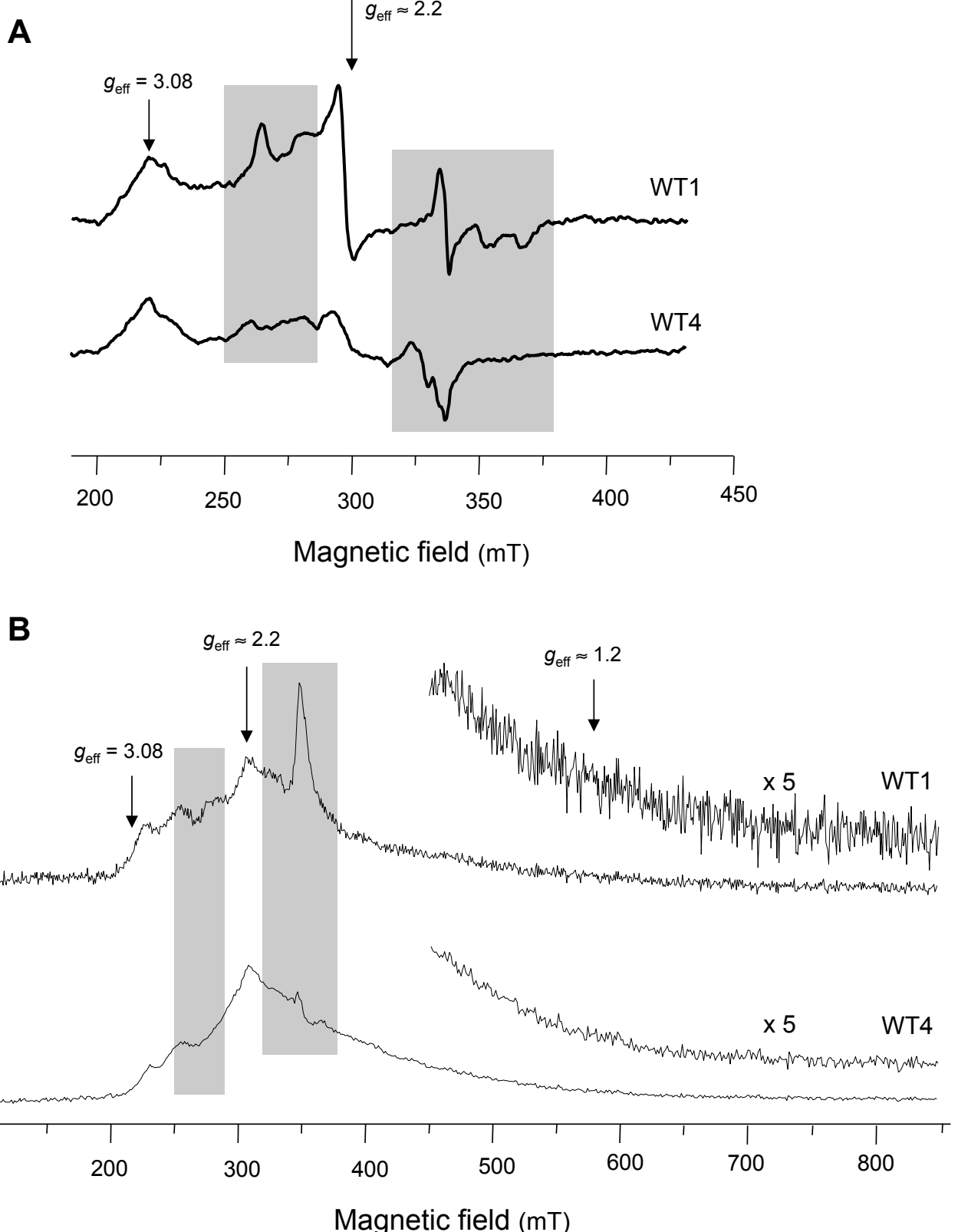


FIGURE S8 | EPR spectra. (A) Continuous-wave (CW) EPR spectra of ferric WT1 and WT4. The spectra were measured at 15 K. Field regions with features corresponding to very minor populations of other low spin and heme-NO forms are shadowed. Positions and the effective g (g_{eff}) values of the signals associated to the HALS center are marked (see text). (B) 3p ei-EPR spectra of ferric WT1 and WT4. The shape of the spectra is similar to the CW-EPR one in absorption mode. Field regions with features corresponding to very minor populations of other low spin and heme-NO forms are shadowed. Positions and the g_{eff} values of the signals associated to the HALS center are marked. Position corresponding to the lowest g principal value (g_x) cannot be detected in CW-EPR spectra as it would display a very broad feature. It was determined in the ei-EPR spectra by the presence of echo at high field values (see text).

TABLE S1 | RNA-sequencing values of the four splice forms of the *MtGlb1-2* gene in various plant organs.

	<i>MtGlb1-2.1</i>			<i>MtGlb1-2.2</i>			<i>MtGlb1-2.3</i>			<i>MtGlb1-2.4</i>		
	R1	R2	R3									
Root	0.51	1.38	2.85	4.49	7.13	7.70	0.11	0.65	1.03	0.00	1.63	0.55
Leaf	0.15	0.00	0.36	1.60	0.00	0.66	0.25	0.00	0.27	0.12	0.00	0.61
Small pod	0.00	0.00	0.00	0.00	0.00	0.00	0.00	0.00	0.00	0.00	0.40	0.00
Medium pod	0.43	0.00	0.00	0.50	0.00	0.03	0.35	0.00	0.04	0.00	0.00	0.00
Large pod	0.00	0.00	0.00	0.35	0.34	0.00	0.39	0.05	0.70	0.00	0.00	0.25
Nod0	0.18	0.00	0.46	1.27	1.07	1.61	1.50	0.28	0.18	0.00	0.00	0.00
Nod4	0.13	0.00	0.00	1.74	0.43	0.00	0.15	0.25	0.39	0.15	0.00	0.00
Nod10	0.00	0.00	0.23	1.71	0.00	0.42	0.05	0.00	0.19	0.00	0.00	0.00
Nod14	0.16	0.00	0.51	0.42	1.45	0.89	0.41	0.16	0.66	0.00	0.14	0.21
Nod28	0.17	0.21	0.00	1.11	0.38	1.00	0.39	0.49	0.24	0.00	0.00	0.16
Nod14 + 12 h	1.21	0.58	0.35	2.78	2.16	1.25	1.21	0.14	0.91	0.64	0.00	0.00
Nod14 + 48 h	0.00	0.49	2.28	1.04	0.61	2.00	0.42	0.30	2.63	0.00	0.15	0.24

Data are three biological replicates (R1 to R3) and correspond to the means and SE's given in Figures 1C and D. Values are expressed in fragments per kilobase of transcript per million reads mapped (FPKM). Nod0 are roots before inoculation; Nod 4 are root bumps at 4 days post-inoculation (dpi); Nod10, Nod14 and Nod28 are nodules at 10, 14 and 28 dpi; and Nod14 + 12 h and Nod14 + 48 h are nodules at 14 dpi that were treated for 12 h and 48 h with 10 mM KNO₃, respectively. Nod, nodules of 4, 10, 18 or 28 days of age.